Synthesis and Electrochemical, Photophysical, and Anion Binding Properties of Self-Assembly Heterometallic Cyclophanes

Shih-Sheng Sun, Jason A. Anspach, Alistair J. Lees,* and Peter Y. Zavalij

Institute for Materials Research and Department of Chemistry, State University of New York at Binghamton, Binghamton, New York 13902-6016

Received October 17, 2001

A series of heterometallic cyclophanes have been prepared from self-assembly of *cis*-(dppf)M$(H_2O)_2(OTf)_2$ (M = Pd or Pt) and $BrRe(CO)_3(L)_2$ with the general formula [*cis*-(dppf)M-(μ-L)$_2$Re$(CO)_3$Br]$_2(OTf)_4$ (**4**: M = Pd, L = 4,4′-bpy; **5**: M = Pt, L = 4,4′-bpy; **6**: M = Pd, L = 1,2-(4′-dipyridyl)acetylene (DPA); **7**: M = Pd, L = 1,4-(4′-dipyridyl)butadiyne (DPB); **8**: M = Pt, L = DPB) or *cis*-(dppf)Pt(4-ethynylpyridine)$_2$ and $BrRe(CO)_5$ with the formula {[*cis*-(dppf)Pt(4-ethynylpyridyl)$_2$](*fac*-Re$(CO)_3$Br)}$_2$ (**10**). These complexes have been characterized by a variety of analytical techniques including IR, NMR, elemental analysis, mass spectrometry, and single-crystal X-ray diffraction. The photophysical properties of these complexes have been examined in detail. Squares **4**−**8** exhibit room-temperature luminescence from lowest-lying triplet-centered metal to ligand charge transfer (^{3}MLCT) excited states, albeit significantly weaker than that predicted on the basis of their excited state energies and the energy gap law. No luminescence was observed from the neutral square **10**. Pd(II)- or Pt(II)-based oxidative quenching and energy transfer pathways from the emitting ^{3}MLCT state to lower nonemissive excited states localized on the ferrocenyl moieties are invoked to explain the luminescence observations. Inorganic anion binding studies for squares **4**−**8** again reveal two different quenching pathways.

Downloaded by CARLI CONSORTIUM on June 29, 2009
Published on January 24, 2002 on http://pubs.acs.org | doi: 10.1021/om0109096

Introduction

The design and formation of thermodynamically driven molecular squares through metal coordination to ligands with predefined size and geometry have been intensely studied in the past decade.[1] The incorporation of photoactive chromophores into the molecular entities is particularly attractive for the development of photonic or electronic devices because of their high sensitivity to changes in the environment.[2] Polypyridyl rhenium(I) and ruthenium(II) complexes have drawn a lot of attention recently; this is due to the ease of their preparation, their tunable luminescent properties, and their potential application in solar energy conversion.[3] Recently, Hupp and co-workers,[4] several other groups,[5] and ourselves[6] have prepared a variety of self-assembly metallocyclophanes or cages comprising rhenium(I) tricarbonyl or dicarbonyl moities with pyridyl or phosphine bridging ligands. Apart from their intriguing structures, many of these metallocyclophanes or cages are luminescent in solution. Moreover, some of them have been found to be effective molecular hosts for anions[4a,f] and certain aromatic compounds[4g−j,5h,6c,d] as a consequence of Coulombic and/or hydrophobic interactions between the host and guest molecules.[7]

* Corresponding author. E-mail: alees@binghamton.edu. Fax: (+1)607-777-4478.

(1) Recent reviews on transition-metal-based self-assembly systems: (a) Leininger, S.; Olenyuk, B.; Stang, P. J. *Chem. Rev.* **2000**, *100*, 853. (b) Swiegers, G. F.; Malefetse, T. J. *Chem. Rev.* **2000**, *100*, 3483. (c) Caulder, D. L.; Raymond, K. N. *J. Chem. Soc., Dalton Trans.* **1999**, 1185. (d) Fujita, M. *Chem. Soc. Rev.* **1998**, *27*, 417. (e) Dinolfo, P. H.; Hupp, J. T. *Chem. Mater.* **2001**, *13*, 3113.

(2) De Silva, A. P.; Gunaratne, H. Q. N.; Gunnlaugsson, T.; Huxley, A. J. M.; McCoy, C. P.; Rademacher J. T.; Rice, T. E. *Chem. Rev.* **1997**, *97*, 1515, and references therein.

(3) (a) Lees, A. J. *Chem. Rev.* **1987**, *87*, 711. (b) Schanze, K. S.; MacQueen, D. B.; Perkins, T. A.; Cabana, L. A. *Coord. Chem. Rev.* **1993**, *122*, 63. (c) Sauvage, J.-P.; Collin, J.-C.; Chambron, S.; Guillerez, C.; Coudret, V.; Balzani, V.; Barigelletti, F.; De Cola, L.; Flamigni, L. *Chem. Rev.* **1994**, *94*, 993. (d) Balzani, V.; Juris, A.; Venturi, M.; Campagna, S.; Serroni, S. *Chem. Rev.* **1996**, *96*, 759.

(4) (a) Slone, R. V.; Yoon, D. I.; Calhoun, R. M.; Hupp, J. T. *J. Am. Chem. Soc.* **1995**, *117*, 11813. (b) Slone, R. V.; Hupp, J. T.; Stern, C. L.; Albrecht-Schmitt, T. E. *Inorg. Chem.* **1996**, *35*, 4096. (c) Slone, R. V.; Hupp, J. T. *Inorg. Chem.* **1997**, *36*, 5422. (d) Benkstein, K. D.; Hupp, J. T.; Stern, C. L. *Inorg. Chem.* **1998**, *37*, 5404. (e) Slone, R. V.; Benkstein, K. D.; Belanger, S. Hupp, J. T.; Guzei, I. A.; Rheingold, A. L. *Coord. Chem. Rev.* **1998**, *171*, 221. (f) Benkstein, K. D.; Hupp, J. T.; Stern, C. L. *J. Am. Chem. Soc.* **1998**, *120*, 12982. (g) Bélanger, S.; Hupp, J. T.; Stern, C. L.; Slone, R. V.; Watson, D. F.; Carrell, T. G. *J. Am. Chem. Soc.* **1999**, *121*, 557. (h) Bélanger, S.; Hupp, J. T. *Angew. Chem., Int. Ed.* **1999**, *38*, 2222. (i) Keefe, M. H.; Slone, R. V.; Hupp, J. T.; Czaplewski, K. F.; Snurr, R. Q.; Stern, C. L. *Langmuir* **2000**, *16*, 3964. (j) Benkstein, K. D.; Hupp, J. T.; Stern, C. L. *Angew. Chem., Int. Ed.* **2000**, *39*, 2891.

(5) (a) Woessner, S. M.; Helms, J. B.; Shen, Y.; Sullivan, B. P. *Inorg. Chem.* **1998**, *37*, 5406. (b) Woessner, S. M.; Helms, J. B.; Houlis, J. F.; Sullivan, B. P. *Inorg. Chem.* **1999**, *38*, 4380. (c) Leadbeater, N. E.; Cruse, H. A. *Inorg. Chem. Commun.* **1999**, *2*, 93. (d) Hong, B. *Comments Inorg. Chem.* **1999**, *20*, 177. (e) Rajendran, T.; Manimaran, B.; Lee, F.-Y.; Lee, G.-H.; Peng, S.-M.; Wang, C. M.; Lu, K.-L. *Inorg. Chem.* **2000**, *39*, 2016. (f) Manimaran, B.; Rajendran, T.; Lu, Y.-L.; Lee, G.-H.; Peng, S.-M.; Lu, K.-L. *Eur. J. Inorg. Chem.* **2001**, 633. (g) Manimaran, B.; Rajendran, T.; Lu, Y.-L.; Lee, G.-H.; Peng, S.-M.; Lu, K.-L. *J. Chem. Soc., Dalton Trans.* **2001**, 515. (h) Xu, D.; Khin, K. T.; van der Veer, W. E.; Ziller, J. W.; Hong, B. *Chem. Eur. J.* **2001**, *7*, 2425.

(6) (a) Sun, S.-S.; Lees, A. J. *Inorg. Chem.* **1999**, *38*, 4181. (b) Sun, S.-S.; Silva, A. S.; Brinn, I. M.; Lees, A. J. *Inorg. Chem.* **2000**, *39*, 1344. (c) Sun, S.-S.; Lees, A. J. *J. Am. Chem. Soc.* **2000**, *122*, 8956. (d) Sun, S.-S.; Lees, A. J. *Chem. Commun.* **2001**, 103. (e) Sun, S.-S.; Lees, A. J. *Inorg. Chem.* **2001**, *40*, 3154.

10.1021/om0109096 CCC: $22.00 © 2002 American Chemical Society
Publication on Web 01/24/2002

Downloaded by CARLI CONSORTIUM on June 29, 2009
Published on January 24, 2002 on http://pubs.acs.org | doi: 10.1021/om0109096

We report herein the preparation and characterization of a series of heterometallic cyclophanes comprising both octahedral and square planar metal components. The successful preparation of heterometallic cyclophanes requires a kinetically inert component that will retain its structural identity, at least at room temperature, and another kinetically labile component which is necessary for the subsequent reversible self-correcting processes before the formation of the final structure. We have found that the incorporation of different transition metals as corner components greatly influences, as well as complicates, the excited state dynamics compared to the homometallic cyclophane analogues.

Experimental Section

Materials and General Procedures. All reactions and manipulations were carried out under N_2 or Ar with the use of standard inert-atmosphere and Schlenk techniques. Solvents used for synthesis were dried by standard procedures and stored under N_2.[8] Solvents used in luminescent and electrochemical studies were spectroscopic and anhydrous grades, respectively. All starting materials are commercially available and used without further purification. The compounds 4-ethynylpyridine,[9] 1,4-(4′-dipyridyl)butadiyne (DPB),[9] (dppf)$PtCl_2$ (dppf is 1,1′-bis(diphenylphosphino)ferrocene),[10] (dppf)$Pt(H_2O)_2(OTf)_2$ (OTf is trifluoromethanesulfonate),[10] (dppf)$Pd(H_2O)_2(OTf)_2$,[10] and *fac*-$BrRe(CO)_3(L)_2$ (**1**, L = 4,4′-bpy; **2**, L = DPB)[6c,11] were prepared according to published procedures. The compound 1,2-(4′-dipyridyl)acetylene (DPA) was obtained as a generous gift from Prof. Jon Zubieta at Syracuse University. Tetrabutylammonium hexafluorophosphate (TBAH) used as supporting electrolyte was rigorously dried (under vacuum at 100 °C for 24 h) prior to use. Nitrogen or argon used for the synthesis and purging experiments was dried and deoxygenated according to a previously reported method.[12]

Equipment and Procedures. NMR spectra were obtained using a Brücker AM 360 spectrometer or a Brücker AC 300 spectrometer. ^{1}H NMR spectra are reported in ppm relative to the proton resonance resulting from incomplete deuteration of the NMR solvent. ^{31}P NMR spectra are reported in ppm relative to external 85% H_3PO_4 at 0.00 ppm. Infrared spectra were measured on a Nicolet 20SXC Fourier transform infrared spectrophotometer. The electrospray ionization mass spectrometry (ESI-MS) experiments were performed on a Hewlett-Packard 1100 MSD electrospray mass spectrometer. Fast atom bombardment (FAB) mass spectra were obtained on a Finnigan Mat 95 mass spectrometer. Elemental analyses were performed by Oneida Research Service, Whitesboro, NY. UV−vis spectra were obtained using a HP 8450A diode array spectrophotometer. Emission spectra and emission lifetimes were recorded in deoxygenated solvent solution at 293 K with an SLM 48000S lifetime fluorescence spectrophotometer equipped with a red-sensitive Hamamatsu R928 photomultiplier tube. The detailed procedures for luminescence and lifetime experiments have been described in a previous paper.[4c]

Bimolecular Stern−Volmer quenching analyses were performed by titration of the Re(I)-corner complexes with the Pd(II)- or Pt(II)-corner complexes. For the Re(I)-corner complexes with DPB or DPA as ligands, the compounds (dppf)M(4-ethylpyridine)$_2$(OTf)$_2$ (M = Pd or Pt) were used as quenchers. For the Re(I)-corner complex with 4,4′-bpy as ligand, (dppf)M(4-phenylpyridine)$_2$(OTf)$_2$ (M = Pd or Pt) were used as quenchers.

Electrochemical measurements were recorded on a Princeton Applied Research Model 263A potentiostat (EG&G instruments). The electrochemical cell consisted of a platinum working electrode, a platinum wire counter electrode, and a $Ag/AgNO_3$ (0.01 M in CH_3CN solution) reference electrode. Cyclic voltammograms were obtained in deoxygenated anhydrous CH_3CN or DMF with the electroactive material (5.0×10^{-4} M) and 0.1 M TBAH as supporting electrolyte. Ferrocene (Fc) was used as an internal standard for both potential calibration and reversibility criteria. All potentials for the complexes in the study are reported relative to Fc/Fc^+. The scan rate was 200 mV/s, and the measurements were uncorrected for liquid-junction potentials.

Inorganic anion binding studies for the Re(I)-based squares were conducted in acetone solution using luminescence detection. A 0.1 mM stock solution of the square complex in acetone was prepared, and a 2 mL portion was transferred to a 1 cm fluorescent cell. A 10 mM solution of the anion in acetone was made using the stock solution of the square complex, and small aliquots were added to the cell. The changes in luminescence intensity were monitored as a function of anion concentration.

Aromatic guest binding studies using a ^{1}H NMR titration procedure were conducted in acetone-d_6. The square complex (∼2 mM) was titrated by addition of the solution of the guest molecule prepared in a stock solution of the square complex. The observed chemical shifts (α or β protons of pyridine) were then monitored as a function of guest concentration.

Synthesis. *fac*-$BrRe(CO)_3(DPA)_2$ (3). To 100 mL of nitrogen-degassed isooctane was added 133 mg (0.33 mmol) of $BrRe(CO)_5$ and 236 mg (1.31 mmol) of DPA, and the resulting mixture was stirred at 60 °C under nitrogen for 4 h. The forming yellow precipitate was collected on the frit while the solution was still hot and washed with isooctane (20 mL × 3) and dried in vacuo. Yield: 90%. IR (ν_{CO}, cm^{-1}, CH_2Cl_2): 2028, 1928, 1893. ^{1}H NMR (300 MHz, DMSO-d_6): 8.77 (d, 4H, H_αPy-Re, $^3J_{H-H}$ = 6.6 Hz), 8.69 (d, 4 H, H_αPy, $^3J_{H-H}$ = 6.0 Hz), 7.75 (d, 4 H, H_β-Re, $^3J_{H-H}$ = 6.7 Hz), 7.61 (d, 4 H, H_βPy, $^3J_{H-H}$ = 6.0 Hz). Anal. Calcd for $BrC_{27}H_{16}N_4O_3Re$: C, 45.64; H, 2.27; N, 7.88. Found: C, 45.60; H, 2.26; N, 7.50.

General Procedure for Synthesis of the Square Complexes Cyclobis{[*cis*-(dppf)M](*μ*-4,4′-bpy)$_2$(*fac*-$Re(CO)_3Br$)}-$(OTf)_4$ (M = Pd or Pt).[5a] To a 100 mL flask containing 0.1 mmol of [M(dppf)$(H_2O)_2$](OTf)$_2$ and 0.1 mmol of *fac*-$BrRe(CO)_3$-(4,4′-bpy)$_2$ was added 30 mL of dried CH_2Cl_2, and the resulting mixture was stirred at room temperature under nitrogen for 24 h. A copious amount of precipitate gradually appeared during this period. The precipitate was collected on a frit, washed with cold CH_2Cl_2, and dried under vacuum to afford an analytically pure product.

Cyclobis{[*cis*-(dppf)Pd](*μ*-4,4′-bpy)$_2$(*fac*-$Re(CO)_3Br$)}-$(OTf)_4$ (4). Yield: 87%. IR (ν_{CO}, cm^{-1}, CH_3NO_2): 2027, 1924, 1897. ^{1}H NMR (360 MHz, CD_3NO_2): 8.81 (d, 8H, H_αPy-Re, $^3J_{H-H}$ = 6.6 Hz), 8.58 (br, 8 H, H_αPy-Pd), 7.93 (m, 16 H, H_o-PhP), 7.73 (m, 8 H, H_p-PhP), 7.62 (m, 16 H, H_m-PhP), 7.42 (d, 8 H, H_βPy-Re, $^3J_{H-H}$ = 6.8 Hz) 7.38 (d, 8 H, H_βPy-Pd, $^3J_{H-H}$ = 5.8 Hz), 4.81 (s, 8 H, H_α-ferr), 4.74 (s, 8 H, H_β-ferr). ^{31}P NMR (CD_3NO_2): 36.1 (s). Anal. Calcd for $C_{118}H_{88}N_8Br_2F_{12}O_{18}P_4S_4Fe_2Pd_2Re_2$: C, 43.71; H, 2.74; N, 3.46. Found: C, 43.91; H, 2.58; N, 3.11. ESI-MS (*m*/*z*): 1546.8 ($[M + H^+ - OTf^-]^{2+}$, calcd *m*/*z* 1545.9).

Cyclobis{[*cis*-(dppf)Pt](*μ*-4,4′-bpy)$_2$(*fac*-$Re(CO)_3Br$)}-$(OTf)_4$ (5). Yield: 79%. IR (ν_{CO}, cm^{-1}, CH_3NO_2): 2027, 1924, 1896. ^{1}H NMR (360 MHz, CD_3NO_2): 8.81 (d, 8H, H_αPy-Re, $^3J_{H-H}$ = 6.8 Hz), 8.60 (d, 8 H, H_αPy-Pt, $^3J_{H-H}$ = 4.2 Hz), 7.93 (m, 16 H, H_o-PhP), 7.71 (m, 8 H, H_p-PhP), 7.59 (m, 16 H, H_m-PhP), 7.42 (dd, 16 H, H_βPy-Re, Pt), 4.80 (s, 8 H, H_α-ferr), 4.70 (s, 8 H, H_β-ferr). ^{31}P NMR (CD_3NO_2): 5.77 (t, $^1J_{Pt-P}$ = 3385 Hz). Anal. Calcd for $C_{118}H_{88}N_8Br_2F_{12}O_{18}P_4S_4Fe_2Pt_2Re_2$: 41.44;

(7) Lehn, J.-M. *Supramolecular Chemistry*; VCH Publishers: New York, 1995.
(8) Perrin, D. D., Armarego, W. L. F., Perri, D. R., Eds. *Purification of Laboratory Chemicals*, 2nd ed.; Pergamon Press: Oxford, U.K., 1980.
(9) Ciana, L. D.; Haim, A. *J. Heterocycl. Chem.* **1984**, *21*, 607.
(10) Stang, P. J.; Olenyuk, B.; Fan, J.; Arif, A. M. *Organometallics* **1996**, *15*, 904.
(11) Wrighton, M. S.; Giordano, P. J. *J. Am. Chem. Soc.* **1979**, *101*, 2888.

Downloaded by CARLI CONSORTIUM on June 29, 2009
Published on January 24, 2002 on http://pubs.acs.org | doi: 10.1021/om0109096

H, 2.59; N, 3.28. Found: C, 41.02; H, 2.62; N, 2.99. ESI-MS (*m*/*z*): 1560.4 ([M − 2 OTf^-]$^{2+}$, calcd *m*/*z* 1560.0).

General Procedure for Synthesis of the Square Complexes Cyclobis{[*cis*-(dppf)M](*μ*-L)$_2$(*fac*-Re(CO)$_3$Br)}(OTf)$_4$ (M = Pd or Pt, L = DPA or DPB). To a 50 mL flask containing 0.10 mmol of *fac*-$BrRe(CO)_3(L)_2$ and 0.10 mmol of (dppf)M$(H_2O)_2(OTf)_2$ was added 20 mL of N_2-purged CH_3NO_2. The resulting dark red solution was stirred at room temperature for 24 h. Subsequently, 200 mL of cold ether was added to rapidly precipitate a dark red solid. The solid was redissolved in 5 mL of CH_3NO_2, and slow diffusion of ether vapor into the concentrated CH_3NO_2 solution resulted in the formation of crystalline solids. These solids rapidly collapsed to an amorphous powder when they were filtered from the solvent.

Cyclobis{[*cis*-(dppf)Pd](*μ*-DPA)$_2$(*fac*-Re(CO)$_3$Br)}(OTf)$_4$ (6). Yield: 42%. IR (ν_{CO}, cm^{-1}, CH_3NO_2): 2028, 1925, 1897. ^{1}H NMR (300 MHz, CD_3CN): 8.79 (d, 4 H, $^3J_{H-H}$ = 6.5 Hz, H_αPy-Re), 8.50 (bd, 4 H, H_αPy-Pd), 7.78−7.55 (m, 40 H, Ph), 7.50 (d, 4 H, $^3J_{H-H}$ = 6.3 Hz, H_βPy-Re), 7.38 (bd, 4 H, H_βPy-Pd), 4.68 (bs, 16 H, ferr). ^{31}P NMR (CD_3CN): 37.4 (s). Anal. Calcd for $C_{126}H_{88}N_8Br_2F_{12}O_{18}P_4S_4Fe_2Pd_2Re_2$: C, 45.33; H, 2.66; N, 3.36. Found: C, 45.06; H, 2.79; N, 3.64. ESI-MS (*m*/*z*): 1596.3 ([M + H^+ − OTf^-]$^{2+}$, calcd *m*/*z* 1595.5).

Cyclobis{[*cis*-(dppf)Pd](*μ*-DPB)$_2$(*fac*-Re(CO)$_3$Br)}(OTf)$_4$ (7). Yield: 78%. IR (ν_{CO}, cm^{-1}, CH_3NO_2): 2028, 1927, 1898. ^{1}H NMR (360 MHz, CD_3CN): 8.77 (d, 4 H, $^3J_{H-H}$ = 6.7 Hz, H_αPy-Re), 8.46 (d, 4 H, $^3J_{H-H}$ = 5.3 Hz, H_αPy-Pd), 7.71−7.50 (m, 40 H, Ph), 7.51 (d, 4 H, $^3J_{H-H}$ = 6.8 Hz, H_βPy-Re), 7.32 (bd, 4 H, H_βPy-Pd), 4.67 (bs, 16 H, ferr). ^{31}P NMR (CD_3CN): 36.9 (s). Anal. Calcd for $C_{134}H_{88}N_8Br_2O_{18}F_{12}P_4Fe_2S_4Pd_2Re_2$: C, 46.85; H, 2.58; N, 3.26. Found: C, 46.81; H, 2.54; N, 3.05. ESI-MS (*m*/*z*): 1602.4 ([M + H^+ − OTf^- − Br]$^{2+}$, calcd *m*/*z* 1602.5).

Cyclobis{[*cis*-(dppf)Pt](*μ*-DPB)$_2$(*fac*-Re(CO)$_3$Br)}(OTf)$_4$ (8). The preparation of square **8** was performed in CH_3NO_2 solution at 40 °C. Yield: 81%. IR (ν_{CO}, cm^{-1}, CH_3NO_2): 2028, 1926, 1896. ^{1}H NMR (360 MHz, CD_3NO_2): 8.80 (d, 4 H, $^3J_{H-H}$ = 7.2 Hz, H_αPy-Re), 8.47 (d, 4 H, $^3J_{H-H}$ = 4.5 Hz, H_α-Py-Pt), 7.96−7.91 (m, 16 H, H_o-PhP), 7.74 (m, 8 H, H_p-PhP), 7.65−7.62 (m, 16 H, H_m-PhP), 7.52 (d, 4 H, $^3J_{H-H}$ = 6.8 Hz, H_βPy-Re), 7.25 (d, 4 H, $^3J_{H-H}$ = 5.9 Hz, H_βPy-Pt), 4.80 (s, 8 H, H_α-ferr), 4.70 (s, 8 H, H_β-ferr). ^{31}P NMR (CD_3NO_2): 5.84 (t, $^1J_{Pt-P}$ = 3412 Hz). Anal. Calcd for $C_{134}H_{88}N_8Br_2O_{18}F_{12}P_4Fe_2S_4Pt_2Re_2$: C, 44.55; H, 2.46; N, 3.10. Found: C, 44.11; H, 1.98; N, 2.62. ESI-MS (*m*/*z*): 1656.5 ([M − 2 OTf^-]$^{2+}$, calcd *m*/*z* 1656.0).

***cis*-(dppf)Pt(4-ethynylpyridyl)$_2$ (9).** To a solution containing 113 mg (1.1 mmol) of 4-ethynylpyridine in 80 mL of THF at −70 °C was added 0.7 mL of *t*-BuLi (1.7 M in pentane), and the resulting mixture was stirred for 1 h at −70 °C. To this solution was added 385 mg (0.5 mmol) of Pt(dppf)Cl_2 in 50 mL of THF, and the mixture was allowed to warm to room temperature by itself and stirred for 16 h. The solvent was removed under vacuum, and the residue was extracted with CH_2Cl_2 (4 × 50 mL). The CH_2Cl_2 solution was reduced in volume to 5 mL. Diethyl ether was then slowly added to precipitate the pale yellow solid. The solid was collected and dried in vacuo. Yield: 260 mg (56%). ^{1}H NMR (360 MHz, $CDCl_3$): 8.18 (d, 4H, H_αPy, J_{H-H} = 6.0 Hz), 7.78 (m, 8 H, H_o-PhP), 7.78 (m, 4 H, H_p-PhP), 7.37 (m, 8 H, H_m-PhP), 6.61 (d, 4 H, H_βPy, J_{H-H} = 6.0 Hz), 4.34 (s, 4 H, H_α-ferr), 4.18 (s, 4 H, H_β-ferr). Anal. Calcd for $C_{48}H_{36}N_2P_2FePt$: C, 60.45; H, 3.80; N, 2.94. Found: C, 60.89; H, 3.91; N, 2.59.

Cyclobis{[*cis*-(dppf)Pt(4-ethynylpyridyl)$_2$](*fac*-Re(CO)$_3$Br)} (10). To a 100 mL flask containing 95.3 mg (0.1 mmol) of [*cis*-Pt(dppf)(4-ethynylpyridine)$_2$] and 40.6 mg (0.1 mmol) of $BrRe(CO)_5$ was added 30 mL of THF, and the resulting mixture was refluxed for 40 h. A copious amount of yellow precipitate gradually appeared during this period. Subsequently, 50 mL of hexane was added to the solution to force further precipitation. The precipitate was collected on a frit, washed with cold ether, and dried in vacuo. Recrystallization from CH_2Cl_2/hexane afforded a pale yellow powder **10**. Yield: 105 mg (81%). IR (ν_{CO}, cm^{-1}, CH_2Cl_2): 2023, 1918, 1885. ^{1}H NMR (360 MHz, CD_2Cl_2): 8.25 (dd, 8H, H_αPy), 7.76 (m, 16 H, H_o-PhP), 7.40 (m, 24 H, H_p, H_m-PhP), 6.52 (d, 4 H, H_βPy, J_{H-H} = 6.3 Hz), 6.47 (d, 4 H, H_βPy, J_{H-H} = 6.6 Hz), 4.40 (s, 8 H, H_α-ferr), 4.22 (s, 8 H, H_β-ferr). ^{31}P NMR (CD_2Cl_2): 15.1 (t, J_{Pt-P} = 2385 Hz). FAB-MS (*m*/*z*): 2607.9 ([M + H]$^+$, calcd *m*/*z* 2607.0), 2527.6 ([M − Br]$^+$, calcd *m*/*z* 2527.1). Anal. Calcd for $C_{102}H_{72}N_4Br_2O_6P_4Fe_2Pt_2Re_2$: 46.98; H, 2.78; N, 2.15. Found: C, 47.11; H, 2.79; N, 2.33.

(dppf)ML$_2$(OTf)$_2$ (L = 4-phenylpyridine, M = Pd (11), M = Pt (12); L = 4-ethylpyridine, M = Pd (13), M = Pt (14)). The procedures for preparing complexes **11**−**14** are essentially the same; only the preparation of **11** is described here. (dppf)Pd$(H_2O)_2(OTf)_2$ (0.05 mmol) and 4-phenylpyridine (0.1 mmol) were placed in a 25 mL flask. To the flask was added 10 mL of CH_2Cl_2, and the resulting solution was stirred at room temperature for 20 min. The solution was slowly added into 100 mL of rapidly stirring cold hexane. The resulting fine powder was collected on a frit and dried in vacuo to afford an analytically pure compound.

11 (purple): Yield: 85%. ^{1}H NMR (360 MHz, acetone-d_6): 8.86 (bd, 4 H, H_αPy), 8.04−7.99 (m, 8 H, H_o-PhP), 7.74−7.70 (m, 4 H, H_p-PhP), 7.65−61 (m, 8 H, H_m-PhP), 7.57 (d, 4 H, $^3J_{H-H}$ = 6.6 Hz, H_βPy), 7.45−7.41 (m, 10 H, Ph), 4.89 (s, 4 H, H_α-ferr), 4.79 (s, 4 H, H_β-ferr). ^{31}P NMR (acetone-d_6): 34.2 (s). Anal. Calcd for $C_{58}H_{46}N_2O_6F_6P_2FeS_2Pd$: C, 54.88; H, 3.65; N, 2.21. Found: C, 54.95; H, 3.79; N, 2.51.

12 (yellow): Yield: 82%. ^{1}H NMR (300 MHz, acetone-d_6): 8.90 (d, 4 H, $^3J_{H-H}$ = 4.1, H_αPy), 8.03−7.97 (m, 8 H, H_o-PhP), 7.69−7.62 (m, 4 H, H_p-PhP), 7.61−7.55 (m, 12 H, H_m-PhP, H_β-Py), 7.47−7.42 (m, 10 H, Ph), 4.87 (s, 4 H, H_α-ferr), 4.75 (s, 4 H, H_β-ferr). ^{31}P NMR (acetone-d_6): 5.35 (t, $^1J_{Pt-P}$ = 3401 Hz). $C_{58}H_{46}N_2O_6F_6P_2FeS_2Pt$: C, 51.30; H, 3.41; N, 2.06. Found: C, 51.12; H, 3.64; N, 2.51.

13 (purple): Yield: 95%. ^{1}H NMR (300 MHz, acetone-d_6): 8.63 (dd, 4H, $^3J_{H-H}$ = 6.6, $^4J_{P-H}$ = 3.3, H_αPy), 7.98−7.91 (m, 8 H, H_o-PhP), 7.73−7.70 (m, 4 H, H_p-PhP), 7.65−7.59 (m, 8 H, H_m-PhP), 6.99 (d, 4 H, H_βPy, $^3J_{H-H}$ = 5.4 Hz), 4.84 (s, 4 H, H_α-ferr), 4.77 (s, 4 H, H_β-ferr), 2.48 (q, 4 H, $-CH_2CH_3$, $^3J_{H-H}$ = 7.8 Hz), 1.03 (t, 6 H, $-CH_2CH_3$, $^3J_{H-H}$ = 7.6 Hz). ^{31}P NMR (acetone-d_6): 33.8 (s). $C_{50}H_{46}N_2O_6F_6P_2FeS_2Pd$: C, 51.19; H, 3.95; N, 2.39. Found: C, 51.63; H, 4.03; N, 2.65.

14 (yellow): Yield: 92%. ^{1}H NMR (300 MHz, acetone-d_6): 8.67 (dd, 4H, $^4J_{P-H}$ = 3.8, H_αPy), 7.97−7.91 (m, 8 H, H_o-PhP), 7.71−7.67 (m, 4 H, H_p-PhP), 7.62−7.57 (m, 8 H, H_m-PhP), 7.02 (d, 4 H, H_βPy, $^3J_{H-H}$ = 5.9 Hz), 4.82 (s, 4 H, H_α-ferr), 4.73 (s, 4 H, H_β-ferr), 2.50 (q, 4 H, $-CH_2CH_3$, $^3J_{H-H}$ = 7.9 Hz), 1.04 (t, 6 H, $-CH_2CH_3$, $^3J_{H-H}$ = 7.5 Hz). ^{31}P NMR (acetone-d_6): 5.24 (t, $^1J_{Pt-P}$ = 3398 Hz). $C_{50}H_{46}N_2O_6F_6P_2FeS_2Pt$: C, 47.59; H, 3.67; N, 2.22. Found: C, 47.93; H, 3.44; N, 2.38.

Crystallography. Single crystals of square **5** suitable for X-ray crystallography were grown by slow diffusion of ether vapor into a concentrated CH_3NO_2 solution of square **5**. The crystal was measured on a Siemens Smart CCD single-crystal diffractometer.[13a] The crystal structure was determined by the direct method and refined by a least-squares procedure using SHELXS97 and SHELXL97 crystallographic packages.[13b] Experimental and crystallographic parameters are shown in Table 1.

Results and Discussion

Synthetic Strategy and General Properties. Scheme 1 represents the concepts leading to the syn-

(12) Dunwoody, N.; Sun, S.-S.; Lees, A. J. *Inorg. Chem.* **2000**, *39*, 4442.

(13) (a) *SMART* and *SAINT*; Bruker AXS Inc.: Madison, WI, 1999. (b) Sheldrick, G. M. *SHELXS97* and *SHELXL97*; University of Göttingen: Göttingen, Germany, 1997.

Table 1. Experimental and Crystallographic Parameters for Square 5·2CH_3NO_2

formula	$C_{120}H_{94}Br_2F_{12}Fe_2N_{10}O_{22}P_4Pt_2Re_2S_4$
space group	*P*1
a	10.5791(3) Å
b	16.8007(3) Å
c	19.7839(5) Å
α	91.743(1)°
β	94.729(1)°
γ	95.635(1)°
V	3484.78(15) Å^3
Z	1
fw	3542.28
calcd density	1.688 g/cm^3
F(000)	1720
abs coeff, *μ*	4.692 mm^{-1}
radiation	Mo Kα
monochromator	graphite
measurement temp	153 K
scan	*ω*
no. of measured reflns	22 019
R equivalents	0.0273
R σ	0.0643
no. of unique reflns	15 185
no. of observed reflns	11 882
observed criterion	$>2\sigma(I)$
min *h, k, l*	−11, −18, −25
max *h, k, l*	13, 21, 26
min., max. 2*θ*	3, 56.5°
data collection software	Brüker SMART
structure refinement software	Brüker SHELXTL
no. of refined params	792
R_F	0.060
wR_{F2}	0.142
GOF	1.069

Scheme 1

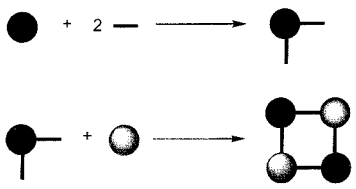

thesis of the heterometallic cyclophanes in this work.[14] The general strategy for preparation of the heterometallic cyclophanes relies on the successful synthesis of the corner component which comprises a thermodynamically inert metal center at room temperature and two uncoordinated donor sites arranged in a *cis*-position.[4a] Subsequent coordination of the donor ligands to another labile metal component, followed by a thermodynamically driven self-assembly process, generates the expected heterometallic cyclophanes. Squares **4**−**8** were prepared according to Scheme 2. By simply mixing equivalent amounts of (dppf)M$(H_2O)_2(OTf)_2$ (M = Pd or Pt) and *fac*-BrRe$(CO)_3(L)_2$ (L = 4,4′-bpy, DPB, or DPA) in CH_2Cl_2 or CH_3NO_2 solution for 24 h, the corresponding squares were isolated with relatively high yields. ^{1}H NMR results showed that the reactions proceeded essentially quantitatively, although typical isolated yields were ca. 80% after collection of the extremely fine powders of the products. Square **6** was particularly difficult to collect on a frit, and it was isolated in only 42% yield. The preparation of squares **6**, **7**, and **8** required the use of CH_3NO_2 as the reaction solvent. When the reactions were performed in CH_2Cl_2, the resultant precipitate comprises several undesirable products that were very difficult to purify; these are presumably various oligomeric or polymeric species. In the case of square **8**, a slightly higher temperature was required to ensure the completion of the reactions.

The synthetic route performed for square **10** is depicted in Scheme 3. The Pt(II)-acetylide corner **9** was prepared from the nucleophilic reaction between the deprotonated 4-ethynylpyridyl carbanion[15] and *cis*-(dppf)$PtCl_2$. The pale yellow Pt(II)-acetylide corner was subsequently refluxed with BrRe$(CO)_5$ in THF for 40 h to afford, after workup, the neutral square **10** in good yield.

Characterization of Squares 4−8. Infrared spectra for squares **4**−**8** comprise three carbonyl stretching bands that are characteristic of the *facial* geometry associated with Re(I) centers.[16] No significant differences in the carbonyl stretching frequencies were observed among the various square complexes. ^{1}H NMR spectra of these square complexes show the same patterns as the individual components, but the peaks are slightly shifted in their positions. The pyridyl protons of the complexes are downfield shifted compared to those of free ligands due to the dative bonding character of the metal−nitrogen bonding. In the cases of squares **4**−**8**, the α and *β* protons of the pyridines coordinated to Re(I) are more downfield shifted (0.13−0.46 ppm for α protons and 0.04−0.23 ppm for *β* protons) than the ones coordinated to Pd(II) or Pt(II). This is due to the stronger electron-withdrawing nature of BrRe$^{\mathrm{I}}(CO)_3$ compared to (dppf)Pd(II) and (dppf)Pt(II). More significantly, the ^{31}P NMR spectra show a single signal for each of these square complexes, indicative of the highly symmetrical structures. For the Pt(II)-containing squares, the $^1J_{Pt-P}$ coupling constants are observed in the range of 3385−3461 Hz, and these values are comparable to other previously reported (dppf)Pt-containing complexes.[10,17] The ESI-MS data for squares **4**−**8** are strongly supportive of the formation of the square structures with detection of the parent ion in each instance. The obtained crystal structure of **5** unambiguously confirms the square geometry (vide infra).

Characterization of Square 10. The infrared spectrum of square **10** exhibits a typical *facial* tricarbonyl stretching pattern, similar to those observed from squares **4**−**8**. The square structure is established on the basis of the FAB-MS data, which show the parent ion cluster at *m*/*z* 2607.9 $(M + H)^+$. It is interesting to note that the pyridyl protons in the ^{1}H NMR spectrum of square **10** recorded in CD_2Cl_2 display four sets of doublets with equal integrated areas, although only a triplet due to the Pt−P coupling is observed in the ^{31}P NMR spectrum. The splitting of the pyridyl protons implies that the two pyridine rings experience slightly different magnetic environments. Two possible reasons can explain this peak splitting, viz., the restricted

(14) Bassani, D. M.; Lehn, J.-M.; Fromm, K.; Fenske, D. *Angew. Chem., Int. Ed.* **1998**, *37*, 2364.

(15) Whiteford, J. A.; Lu, C. V.; Stang, P. J. *J. Am. Chem. Soc.* **1997**, *119*, 2524.

(16) (a) Wrighton, M. S.; Giordano, P. J. *J. Am. Chem. Soc.* **1979**, *101*, 2888. (b) Worl, L. A.; Duesing, R.; Chen, P.; Ciana, L. D.; Meyer, T. J. *J. Chem. Soc., Dalton Trans.* **1991**, 849.

(17) (a) Longato, B.; Pilloni, G.; Valle, G.; Corain, B. *Inorg. Chem.* **1988**, *27*, 956. (b) Granifo, J.; Vargas, M. E.; Garland, M. T.; Baggio, R. *Inorg. Chim. Acta* **2000**, *305*, 143. (c) Leininger, S.; Fan, J.; Schmitz, M.; Stang, P. J. *Prog. Natl. Acad. Soc.* **2000**, *97*, 1380.

Downloaded by CARLI CONSORTIUM on June 29, 2009
Published on January 24, 2002 on http://pubs.acs.org | doi: 10.1021/om0109096

Downloaded by CARLI CONSORTIUM on June 29, 2009
Published on January 24, 2002 on http://pubs.acs.org | doi: 10.1021/om0109096

Scheme 2

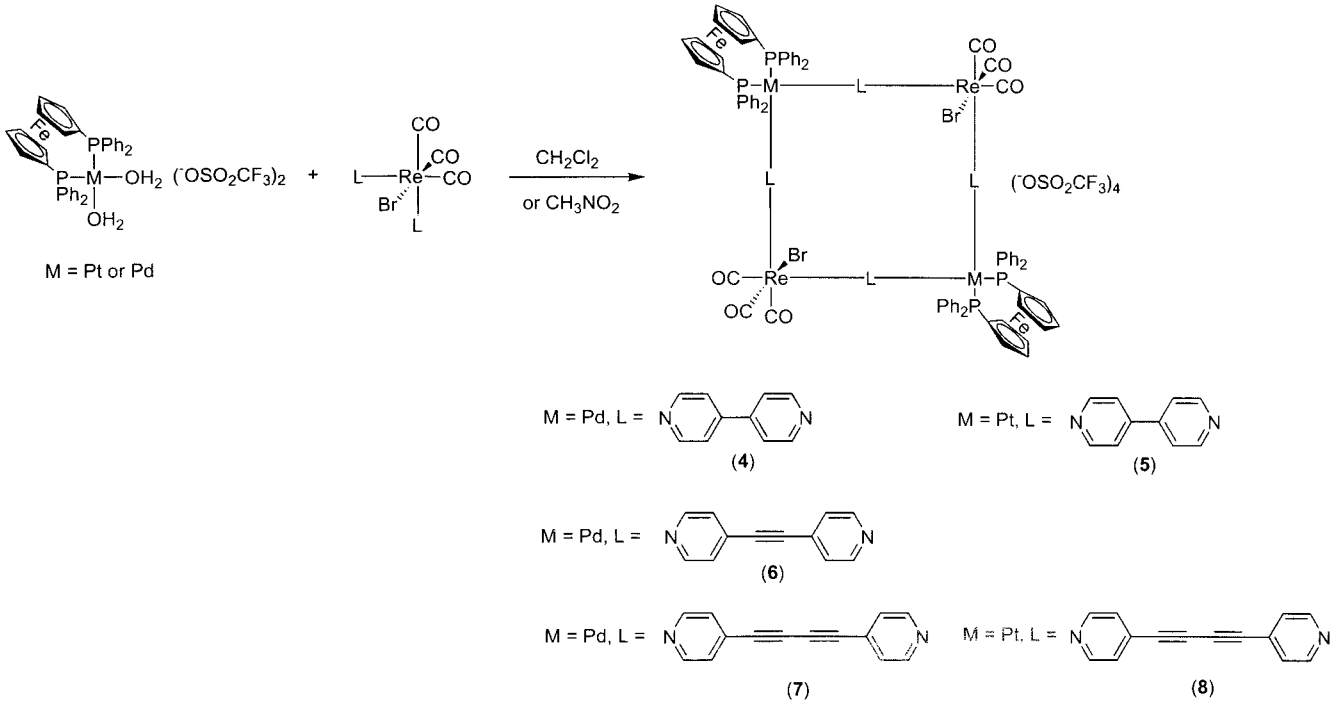

Scheme 3

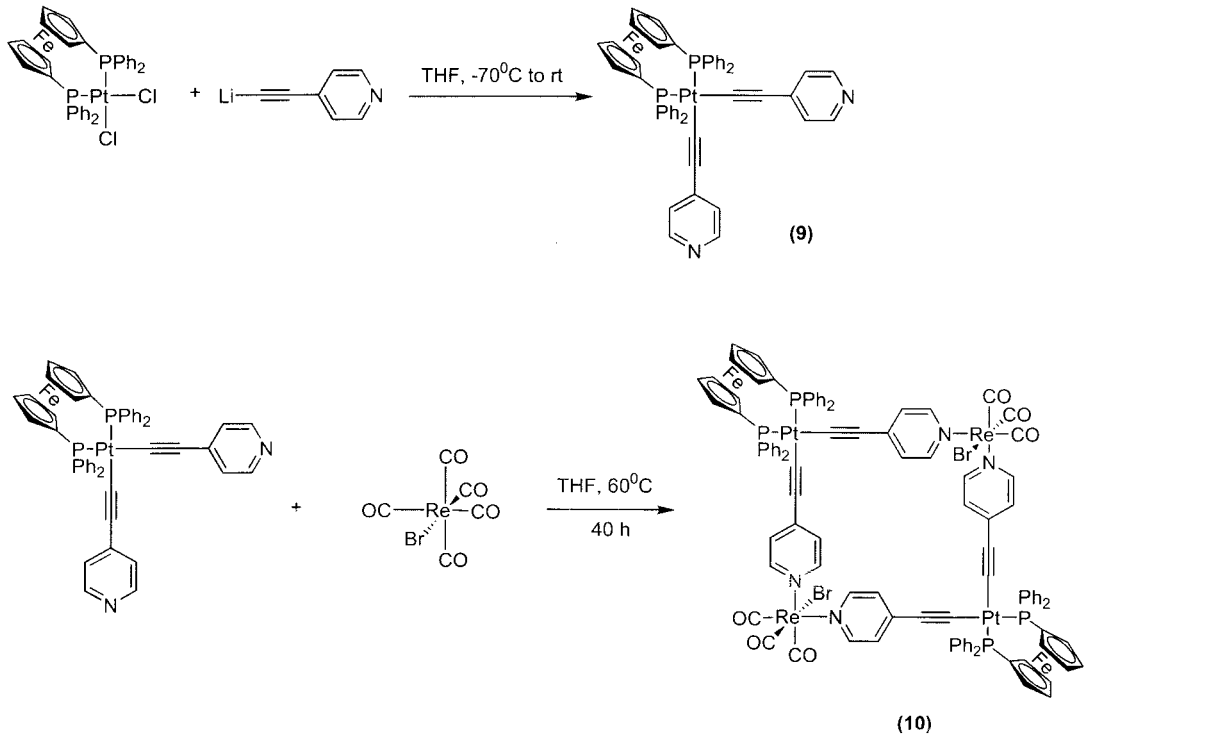

rotation of the pyridyl rings at room temperature or the coexistence of stereoisomers with respect to the relative positions between the Br and CO ligands. The former possibility is excluded on the basis of variable-temperature (263−310 K) ^{1}H NMR experiments in CD_2Cl_2, which showed no sign of coalescence of these peaks. In addition, the crystal structure of square **5** exhibits disorder associated with the Br and CO ligands, and interestingly, there is also the reported observation of two singlets from the nominally equivalent pyrazine protons in the ^{1}H spectrum of square $[ClRe(CO)_3(\mu$-pyrazine$)]_4$ by Hupp et al.[4b] Thus, the coexistence of stereoisomers is understood to be the cause of the two types of pyridyl protons for square **10**.

Crystal Structure of Square 5. The single crystals of square **5** were grown by slow diffusion of ether vapor into a concentrated solution of **5** in CH_3NO_2. The ORTEP diagram of **5** is shown in Figure 1. Selected bond distances and angles as well as torsion angles are given in Tables 2 and 3, respectively. The coordination geometry around the Re center is *facial* with three carbonyl groups, two nitrogen pyridine donors, and one

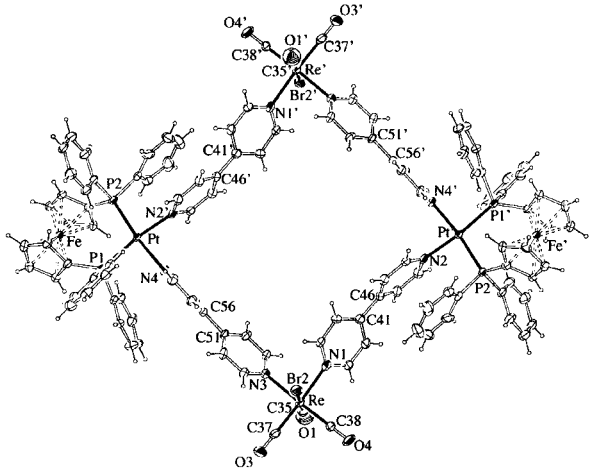

Figure 1. ORTEP diagram of square **5**. Ellipsoids are shown at 50% probability level. The counterions and solvent molecules are not shown for clarity.

Table 2. Selected Bond Distances (Å) and Bond Angles (deg) for Square 5·2CH$_3$NO$_2$

Re−N(1)	2.235(7)	Re−N(3)	2.213(7)
Pt−N(2)	2.095(7)	Pt−N(4)	2.119(7)
Pt−P(1)	2.284(2)	Pt−P(2)	2.289(2)
N(1)−Re−N(3)	84.3(2)	N(2)−Pt−N(4)	83.6(3)
N(2)−Pt−P(2)	89.9(2)	N(4)−Pt−P(1)	88.2(2)
P(1)−Pt−P(2)	99.04(7)		

Table 3. Selected Torsion Angles (deg) for Square 5·2CH$_3$NO$_2$

C(40)	C(41)	C(46)	C(45)	28.9(13)
C(42)	C(41)	C(46)	C(45)	−156.0(9)
C(40)	C(41)	C(46)	C(47)	−144.9(9)
C(42)	C(41)	C(46)	C(47)	30.2(12)
C(50)	C(51)	C(56)	C(55)	35.8(12)
C(52)	C(51)	C(56)	C(55)	−145.8(8)
C(50)	C(51)	C(56)	C(57)	−143.9(9)
C(52)	C(51)	C(56)	C(57)	34.5(12)

bromine atom. The average Re−N bond distance is ∼2.2 Å, which is comparable to related structures reported in the literature.[4b,g,i,18] The average Pt−N bond is ∼2.1 Å, and this is also close to that determined for related Pt(II)-pyridine complexes.[4g,19] The Pt−P bonds and P−Pt−P angles are comparable to reported crystal structures containing (dppf)Pt units.[20] It is found that the stacking effect between the phenyl ring of diphenylphosphinoferrocene and the neighboring pyridyl ring causes a slight distortion from an ideal square structure; the N−Pt−N angle is 83.6° and the N−Re−N angle is 84.3°. A similar stacking effect has also been observed in other reported square crystal structures.[4a,19] Also, the bridging 4,4′-bpy ligands are not flat, and the dihedral angles between its rings are 32°. The dimensions of the cavity, as defined by the distances between Re(I) and Pt(II), are 11.28 × 11.38 Å. It should also be pointed out that the pair of trans Br and CO groups is statistically disordered in a ratio 1:2. Indeed, this halide/CO disorder has also been observed in other crystal structures of square complexes containing *fac*-rhenium tricarbonyl halide moieties.[4b]

Despite the collection of the X-ray data at low temperature, the solvent in this structure is still disordered. From difference Fourier analysis, it was possible to localize four CF_3SO_3 anions and two CH_3NO_2 molecules. However, the displacement parameters of these species were high, so the geometry was fixed throughout the refinement. More solvent peaks were also found but were not identified due to very high thermal displacement parameters; therefore, these were refined as separate carbon atoms (see Supporting Information). The crystal packing pattern for **5** indicates the formation of extended channels with CH_3NO_2 and unidentified solvent molecules filled inside the channels. It is also noticeable that the triflate anions are not located inside the square but are located between the squares.

Electrochemistry. Cyclic voltammetric experiments were performed in CH_3CN or DMF solution at ambient temperature, and the data are presented in Table 4. It can be seen that two oxidation potentials are observed for all the square complexes except for square **10**. On the basis of the oxidation potentials of the Re(I)-based corners and (dppf)Pt$(H_2O)_2(OTf)_2$, the first reversible oxidation process is assigned to $Fe^{2+/3+}$ and the second irreversible oxidation process is assigned to $Re^{1+/2+}$. The $Re^{1+/2+}$ oxidation potential in square **10** was not observed due to the limit of the DMF window in our experimental conditions. The reduction processes observed are assigned to the successive addition of electrons to the π^* orbitals localized in the bridging ligand. In general, the redox potentials between the Pd(II) and Pt(II) squares containing the same bridging ligand do not vary too much, and the reduction potentials shift to a less cathodic position when the bridging ligand is more conjugated, i.e., DPB > DPA > bpy.

Photophysical Properties. The obtained photophysical data, including absorption, emission spectra, lifetimes, and emission quantum yields, of all the square complexes studied are summarized in Table 5. It is noted that the absorption spectra of the squares **4**−**8** and square **10** are very similar to other previously reported Re(I) diimine complexes.[4a,b,6a,c,e,18a] In general, there are two main absorption features in the UV and near UV region for the squares and their Re-corner complexes. The higher energy feature is assigned to a ligand localized IL ($\pi-\pi^*$) absorption, and the lower energy absorption is attributable to a Re ($d\pi$) to ligand (π^*) charge transfer (MLCT) transition.[11] A very weak absorption band centered around 530 nm is assigned to a d−d transition localized on the dppf moiety.[21] Figure 2 compares the absorption spectra of square **7** and its corresponding Re(I)-corner **2** and Pd-corner **13** complexes in CH_2Cl_2 solution. Typically, the MLCT bands of the square complexes are slightly red shifted and the extinction coefficients are roughly twice those of their corresponding Re(I) corner complexes, as anticipated.

Square complexes **4**−**8**, as well as their Re(I)-corner complexes, exhibit luminescence in room-temperature solution, whereas square **10** does not have detectable luminescence in room-temperature CH_2Cl_2 solution. The striking feature of these emitting squares, compared to their corresponding Re(I)-corner complexes, is that the

Downloaded by CARLI CONSORTIUM on June 29, 2009
Published on January 24, 2002 on http://pubs.acs.org | doi: 10.1021/om0109096

(18) (a) Lin, J. T.; Sun, S.-S.; Wu, J. J.; Liaw, Y.-C.; Lin, K.-J. *J. Organomet. Chem*. **1996**, *517*, 217. (b) Bélanger, S.; Hupp, J. T.; Stern, C. L. *Acta Crystallogr*. **1998**, *C54*, 1596.
(19) Stang, P. J.; Cao, D. H.; Saito, S.; Arif, A. M. *J. Am. Chem. Soc.* **1995**, *117*, 6273.
(20) Bandoli, G.; Dolmella, A. *Coord. Chem. Rev*. **2000**, *209*, 161.
(21) (a) Geoffroy G. L.; Wrighton, M. S. *Organometallic Photochemistry*; Academic Press: New York, 1979. (b) Lee, E. J.; Wrighton, M. S. *J. Am. Chem. Soc.* **1991**, *113*, 8562.

Table 4. Redox Potentials[a]

compound	E_{ox}, V	E_{red}, V
$BrRe(CO)_3(bpy)_2$	0.96	−1.95, −2.10
$BrRe(CO)_3(DPB)_2$	1.10 (i)	−1.80 (i), −2.18 (i)
$BrRe(CO)_3(DPA)_2$	1.07 (i)	−1.88 (i)
$[(dppf)Pd(\mu\text{-bpy})_2Re(CO)_3Br]_2(OTf)_4$	0.75, 1.10 (i)	−2.18 (i), −2.41
$[(dppf)Pt(\mu\text{-bpy})_2Re(CO)_3Br]_2(OTf)_4$	0.76, 1.10 (i)	−2.09 (i), −2.41
$[(dppf)Pd(\mu\text{-DPA})_2Re(CO)_3Br]_2(OTf)_4$	0.76, 1.08 (i)	−1.92 (i), −2.38 (i)
$[(dppf)Pd(\mu\text{-DPB})_2Re(CO)_3Br]_2(OTf)_4$	0.76, 1.06 (i)	−1.83 (i), −2.20 (i)
$[(dppf)Pt(\mu\text{-DPB})_2Re(CO)_3Br]_2(OTf)_4$	0.74, 1.12 (i)	−1.77 (i), −2.16 (i)
$[(dppf)Pt(4\text{-ethynylpyridine})_2Re(CO)_3Br]_2$ [b]	0.39	−1.56 (i)
$(dppf)Pd(4\text{-Etpy})_2(OTf)_2$	0.78	
$(dppf)Pt(OH_2)_2(OTf)_2$	0.80	

[a] Analyses were performed in 0.5 mM deoxygenated CH_3CN solutions containing 0.1 M TBAH, scan rate is 200 mV/s. All potentials in volts vs $[Fe(C_5H_5)_2]^{+/0}$ (0.12 V with peak separation 80 mV in DMF and 0.17 V with peak separation 100 mV in CH_3CN); (i) = irreversible process and the reported values are peak positions. [b] DMF solution.

Table 5. Electronic Absorption and Emission Data at 293 K[a]

	absorption spectra	emission[b]		
compd	λ_{max}, nm ($10^{-3}\epsilon$, $M^{-1}cm^{-1}$)	λ_{max}, nm	τ, ns[c]	Φ_{em}
1	248 (35.5), 320 (14.0)	585	1200	0.016
2	251 (47.5), 262 (46.4), 288 (28.4), 302 (31.1), 322 (36.0), 345 (31.5)	612	100	0.0040
3	281 (41.7), 296 (38.3), 326 (20.0)	592	160	0.0083
4	254 (96.0), 337 (32.4), 516 (2.33)	605	9.4	5.82×10^{-4}
5	252 (116), 343 (28.0)	612	8.4	3.65×10^{-4}
6	289 (143), 344 (57.1), 510 (3.52)	610	14.6	4.80×10^{-4}
7	262 (100), 308 (84.5), 327 (94.4), 349 (77.2), 502 (3.99)	628	11.7	4.80×10^{-4}
8	259 (116), 311 (77.7), 328 (87.9), 347 (73.1)	632	9.2	4.02×10^{-4}
10	277 (56.0), 294 (61.5), 323 (81.9)	*d*		
11	282 (60.3), 337 (10.0), 502 (2.52)	*d*		
12	281 (53.4)	*d*		
13	255 (28.7), 288 (21.3), 343 (5.40), 502 (1.16)	*d*		
14	258 (21.2)	*d*		

[a] CH_2Cl_2 solution. [b] λ_{ex} = 360 nm. [c] The errors on the obtained lifetimes for square complexes are estimated to be 20% due to the low emission quantum yields. [d] No detectable emission in room-temperature solution.

Downloaded by CARLI CONSORTIUM on June 29, 2009
Published on January 24, 2002 on http://pubs.acs.org | doi: 10.1021/om0109096

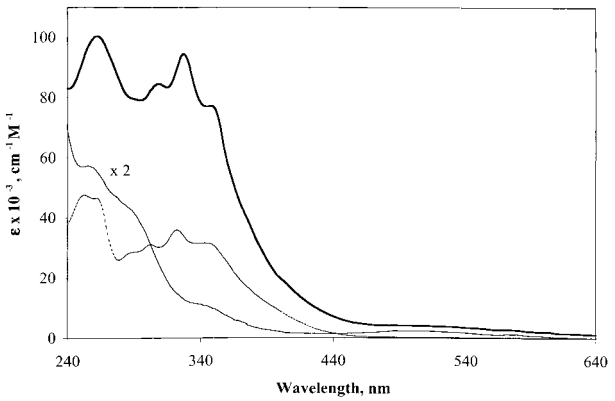

Figure 2. Electronic absorption spectra of square **7** (thick line), Re(I) corner **2** (dashed line), and Pd(II) corner **13** (solid line) in CH_2Cl_2 solution.

squares exhibit band maxima at longer emission wavelengths (416−754 cm^{-1}), shorter lifetimes (7−143-fold), and lower emission quantum yields (8−44-fold) than their corresponding corner complexes. Typically, the luminescent quantum yields of *fac*-tricarbonylrhenium(I) complexes are governed by the rate of nonradiative decay from the emitting ^{3}MLCT state, which is largely determined by the energy gap law.[22] According to this law, the lowest energy emitting excited state is subjected to greater vibrational overlap with the ground state as the energy separation between these levels is reduced; this consequently results in an increase in the nonradiative decay rates. However, the lifetimes determined for squares **4**−**8** are apparently much shorter than predicted on the basis of the energy gap law when one compares them to other *fac*-tricarbonylrhenium complexes.[4a,22] Two structurally similar square complexes of the formula cyclobis{[*cis*-(dppp)M](μ-4,4′-bpy)$_2$-[$Re(CO)_3Cl$]}$(OTf)_4$ (M = Pd or Pt and dppp is 1,3-diphenylphosphinopropane) have been determined to exhibit analogous photophysical properties, and the short lifetimes in these square complexes have been rationalized by invoking intramolecular quenching from the Pd(II)- or Pt(II)-corners.[4a,e]

Table 6. Bimolecular Quenching Constants Derived from Stern−Volmer Analysis between the Re(I)- and Pd(II)- or Pt(II)-Corner Complexes in CH_2Cl_2 Solution at 293 K

complex/quencher	k_q, $M^{-1}s^{-1}$
$BrRe(CO)_3(bpy)_2$/$(dppf)Pd(4\text{-phpy})_2(OTf)_2$	1.2×10^{10}
$BrRe(CO)_3(bpy)_2$/$(dppf)Pt(4\text{-phpy})_2(OTf)_2$	5.9×10^{9}
$BrRe(CO)_3(DPB)_2$/$(dppf)Pd(4\text{-Etpy})_2(OTf)_2$	6.9×10^{9}
$BrRe(CO)_3(DPB)_2$/$(dppf)Pt(4\text{-Etpy})_2(OTf)_2$	1.1×10^{9}
$BrRe(CO)_3(DPA)_2$/$(dppf)Pd(4\text{-Etpy})_2(OTf)_2$	7.8×10^{9}

Table 6 summarizes the bimolecular quenching constants (k_q) determined from Stern−Volmer quenching studies between the individual Re(I)-corner and the Pd(II)- or Pt(II)-corner molecular components. It can be seen that the obtained quenching constants range from 9.2×10^8 to 1.2×10^{10} M^{-1} s^{-1}. Figure 3 shows the Stern−Volmer plot observed for the corner complexes **3** and **13**, confirming that there is efficient bimolecular

(22) Caspar, J.; Meyer, T. J. *J. Phys. Chem.* **1983**, *87*, 952. According to the data reported in this reference, an 1100 cm^{-1} decrease in E_{00} will cause a roughly 5-fold increase in the nonradiative rate constant. Hence, the lifetimes of the square complexes in our work exhibit values of only about 20% of that predicted by the energy gap law.

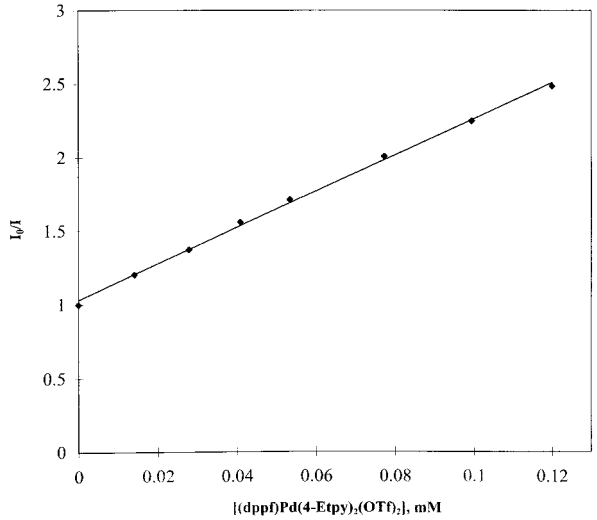

Figure 3. Stern−Volmer plot of the bimolecular emission quenching between the Re(I) corner **3** and the Pd(II) corner **13** complexes in CH_2Cl_2 solution at 293 K.

Scheme 4

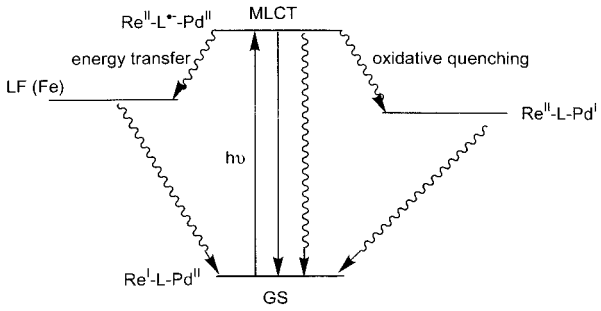

quenching between the Re(I) and Pd(II) or Pt(II) corners. This plot is representative for all of our quenching data. In our square complexes, however, the lifetime data (vide supra) illustrate an even more effective quenching process taking place, which is probably the result of the incorporation of the ferrocenyl moieties in the Pd or Pt corners. It seems unlikely, though, that the increased quenching efficiency is solely due to oxidative electron transfer from the bridging ligand radical anion π^* orbital to the Pd(II) or Pt(II) corners. Given the fact that dppf is a better electron donor than dppp, this should provide a stronger electrostatic stabilization of the positively charged metal center (Pd or Pt) and, thus, decrease the exothermicity of the oxidative quenching process. Alternatively, we note that there is a partial overlap between the absorption spectrum of (dppf)M(4-phenylpyridine)$_2$(OTf)$_2$ (M = Pd or Pt) or (dppf)M(4-ethylpyridine)$_2$(OTf)$_2$ (M = Pd or Pt) and the emission spectra of both the square and Re(I)-corner complexes. This observation strongly suggests that the quenching is also influenced by intramolecular energy transfer from the ^{3}MLCT excited state to lower ferrocene-based metal-center (^{1,3}MC) states.[21] A qualitative energy diagram portraying the photophysical processes occurring in the square molecules is depicted in Scheme 4.

As noted above, square **10** does not display detectable emission at room temperature, and this is also attributed to the quenching effect exerted from the (dppf)Pt(II) moieties. In this case, there is a relatively short distance between the Re(I) chromophores and (dppf)Pt(II). Additionally, the σ-bonding character of the Pt(II)-acetylide system is expected to provide a better orbital overlap between the (dppf)Pt(II) and 4-ethynylpyridine moieties (compared to (dppf)Pt(II) and bipyridyl ligands in squares **4**−**8**). Both of these aspects will enhance the efficiency of intramolecular energy and electron transfer in square **10**.

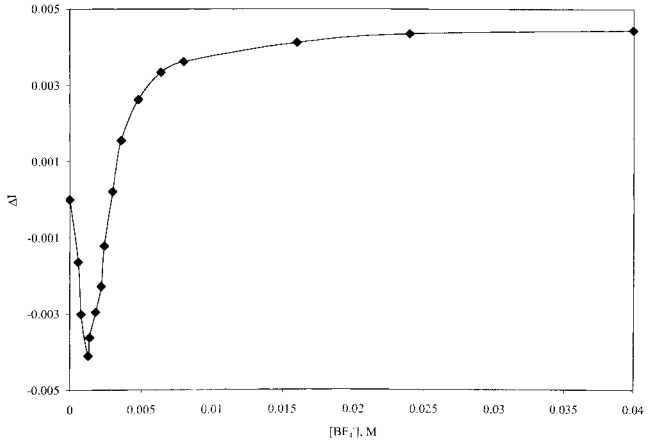

Figure 4. Binding isotherm depicting change of emission of square **4** upon addition of ^{n}Bu$_4$BF$_4$ in acetone solution.

Anion Binding Studied by Luminescence. Anion sensing chemistry has become one of the most intriguing fields of supramolecular chemistry owing to its fundamental role in many chemical and biological processes.[23] The well-defined structures and positive charges associated with the squares studied here render them as potentially effective hosts for anionic species. The fact that several of the squares are also luminescent is an additional feature that may facilitate their development as sensor molecules.

Binding studies between squares **4**−**8** and different inorganic anions were carried out in acetone solution. Among the anions we investigated, viz., ClO_4^-, OAc^-, OTf^-, PF_6^-, and BF_4^-, only the latter two induced significant changes in the luminescence intensities of squares **4**−**8** upon addition. The binding behaviors of the BF_4^- and PF_6^- anions in acetone solution are quite unusual. Figure 4 shows a representative binding curve between the BF_4^- anion and square **4**. The luminescence intensity first *decreases* when a small amount of BF_4^- is added to 0.1 mM square **4** in acetone solution. When the amount of added BF_4^- apparently rises over a critical concentration, the luminescence intensity then starts to *increase* and finally reaches a plateau. Similar results were also observed for the PF_6^- anion as well as for the other luminescent squares **5**−**8**. The unusual changes of the emission intensity upon addition of BF_4^- or PF_6^- also indicate that these are not just simple anion exchange processes.

The results strongly suggest that two different quenching pathways are responsible for the decay of the excited state and that these pathways compete with one another. It should be noted that the emission position and band shape do not change with the anion binding, which suggests an indirect electronic perturbation on the Re(I) chromophores. The initial binding of BF_4^- to the square complex is expected to cause a red shift of the ferrocenyl LF band and, thus, increase the probability of energy transfer from the ^{3}MLCT state to ^{1,3}LF states.

(23) Schmidtchen, F. P.; Berger, M. *Chem. Rev.* **1997**, *97*, 1609.

Downloaded by CARLI CONSORTIUM on June 29, 2009
Published on January 24, 2002 on http://pubs.acs.org | doi: 10.1021/om0109096

The result is a decrease in the luminescence intensity. When more BF_4^- is added into the solution, the excess anions start to stabilize the positive charges on Pd(II) and reduce the oxidative quenching probability, and thus, the luminescence intensity is increased.

The physical basis of why only BF_4^- and PF_6^- induce the change in the luminescence of the square complexes deserves further investigation with other systems. Presumably this relates to the anion encapsulation inside the square cavity and the electrostatic induced ion-pair interaction between the square and anion. The involvement of the solvent's dielectric property and the polarizability of the anions are also expected to play significant roles in these host−guest interactions.

Aromatic Guest Binding Studied by ^{1}H NMR Titration. The aromatic guest binding studies were conducted in acetone-d_6 for squares **4**−**8** and CD_3CN for square **10**. No significant ^{1}H NMR shifts were observed (less than 0.01 ppm for pyridyl protons) for each of these squares when they were mixed with the guest molecules including 1,3,5-trimethoxybenzene, 2-naphthalenesulfonic acid (sodium salt), and 2,6-naphthalenedisulfonic acid (disodium salt). These results suggest that there are little or negligible $\pi-\pi$ or hydrophobic interactions between the guest molecule and the square host.

Conclusions

Two series of heterometallic cyclophanes have been prepared and characterized from self-assembly of *cis*-(dppf)M$(H_2O)_2(OTf)_2$ (M = Pd or Pt) and $BrRe(CO)_3(L)_2$ (L = bis-monodentate pyridyl ligands) or *cis*-(dppf)Pt-(4-ethynylpyridine)$_2$ and $BrRe(CO)_5$. The single-crystal structure of square **5** establishes the dimensions to be 11.28 × 11.38 Å on the edges, based on the Re−Pt interatomic distances. The crystal stacking diagram shows extended channels, which are filled with solvent molecules in the solid state.

The photophysical properties have been shown to be predominantly influenced by the electronic properties of the bridging ligands. No luminescence was observed from neutral square **10**, although squares **4**−**8** that are bridged by rigid or semirigid ligands such as 4,4′-bpy, DPA, and DPB exhibit room-temperature luminescence, albeit weaker than predicted by energy gap law considerations. The low luminescence quantum yields are ascribed to two different quenching pathways, specifically Pd(II)- or Pt(II)-based oxidative quenching and energy transfer from the emitting ^{3}MLCT states to lower nonemissive excited levels localized on the ferrocenyl moieties. Unusual anion binding behavior has been determined, and this is found to be also influenced by these two different quenching mechanisms. ^{1}H NMR titration experiments carried out for several aromatic guest molecules indicate that there are not any strong $\pi-\pi$ association interactions with these squares.

Acknowledgment. We are grateful to the Division of Chemical Sciences, Office of Basic Energy Sciences, Office of Science, U.S. Department of Energy (Grant DE-FG02-89ER14039), for support of this research. We also thank Prof. Omowunmi A. Sadik for access to electrochemical equipment, Dr. Jürgen Schulte for helping acquire ^{31}P NMR spectra, and Prof. Jon Zubieta at Syracuse University for supplying the DPA ligand. The Department of Chemistry of Syracuse University is also acknowledged for access to the X-ray facility for collecting the single-crystal data.

Supporting Information Available: Crystallographic data, in CIF format, and a figure showing the crystal packing diagram (PDF). This material is available free of charge via the Internet at http://pubs.acs.org.

OM0109096

Downloaded by CARLI CONSORTIUM on June 29, 2009
Published on January 24, 2002 on http://pubs.acs.org | doi: 10.1021/om0109096